



INTRODUCTION

Low-echo, spherical lesion phantoms are useful tools for assessing detailed spatial resolution of ultrasound scanners, including those equipped with multi-row, linear and curvilinear arrays, and for tuning system presets for specific applications. Current commercially available lesion phantoms, such as the Sun Nuclear Sono408, with spherical targets arranged in a plane are costly to manufacture and are difficult to use because of the need for precise alignment of the scan plane with the lesion centers. To lower the cost and ease the scan setup process, a new phantom was designed with a mixture of 2mm to 4 mm diameter anechoic spheres randomly distributed over the volume. This project compares the usefulness of this prototype void phantom to the Sono408 for assessing lesion detectability for various transducers and scan setups.

METHOD

Two multi-row, “1.25D” transducers (9L4 on a Siemens S3000; ML6-15-D on a GE Logiq E9) were utilized. For each probe, very similar image settings were used to scan the two phantoms. Five consecutive transmit focal depths starting from the shallowest depth were utilized. For the prototype phantom, multiple scan planes were tested before a plane with ample random lesions was selected for comparison with the Sono408. For the Sono408, both the 2mm diameter and the 4mm diameter spherical lesion areas were scanned. Images using the ML6-15-D probe were acquired using both a single-transmit focus setting and a double-focal-zone setting.

DICOM Images of the 4mm diameter spherical lesions from the Sono408 phantom were used to estimate the elevational thickness of the ultrasound beam profile at various depth. This calculation[1] is based on an estimation of elevational beam width (d) as a function of factors including the radius of the spherical lesion (R), the average echo intensity of a spherical lesion over the B-mode image domain (I_{avg}), the echo signal from the spherical lesion (I_l), the echo signal from the nearby background area adjacent to the spherical lesion (I_b), and the diameter of the spherical lesion relative to the elevational thickness. Moreover, the fact that the lesion’s echogenicity is more than 25 dB lower than that of the background further simplifies the calculation.

RESULTS

Spherical lesions were easily seen in the prototype void phantom, a somewhat more challenging task with the Sono408. Very similar patterns of lesion detectability were observed for the two phantoms using either of the two 1.25D probes. As the focal depth increased, lesion detectability vs depth gradually changed. But the loss of lesion detectability was dramatic beyond a certain transmit focal depth, when the elevational aperture expands significantly due to the sudden engagement of more elevational rows of the 1.25D probe. This phenomenon was apparent using both phantoms, and was especially salient when two focal zones were used (see, for example, the bottom right images of Figure 1 and Figure 2, where the 2mm spherical lesions within the two focal zones were either diminished in contrast with respect to the background area or were barely visible).

Unfortunately, no warning message was given when such abrupt involvement of more elevational rows happened as the user tweaked the focal depth knob near such a transition depth. Clinically this could lead to missing small lesions at this transition depth or erroneous fill-in of small cysts if the sonographer is not aware of the boosted elevational aperture (hence the diminished lesion detectability) beyond this depth. Hence a thorough understanding of how the elevational aperture changes in such a scenario is important when setting up clinical protocols with 1.25 D transducers. Such understanding can be accomplished by quantifying how the elevational thickness changes relative to depth for various transmit focus settings. This can be achieved using images from either the Sono408 phantom or the prototype random void phantom.

RESULTS (CONTINUE)

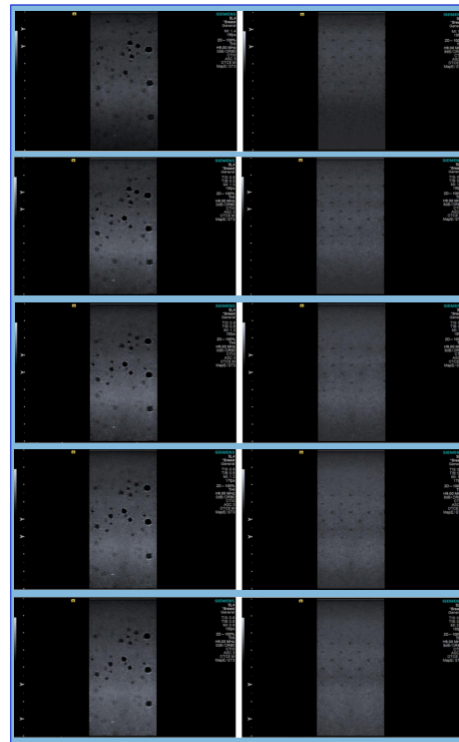


Figure 1. 9L4 on a Siemens S3000 (Left: prototype void phantom; Right: Sono408 phantom. Same scan settings.)

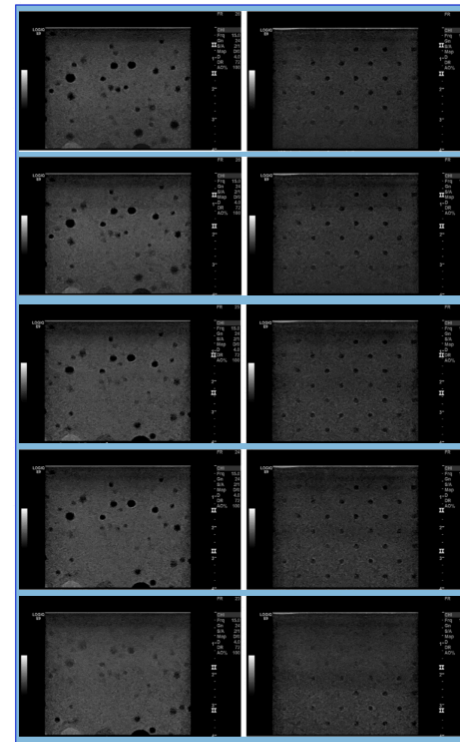


Figure 2. ML6-15-D on a GE Logiq E9, two focal zones (Left: prototype void phantom; Right: Sono408 phantom. Same scan settings.)

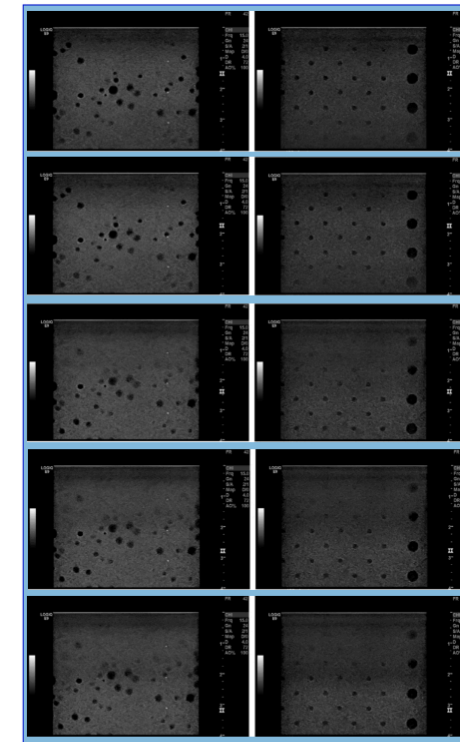


Figure 3. ML6-15-D on a GE Logiq E9, one focal zone (Left: prototype void phantom; Right: Sono408 phantom. Same scan settings.)

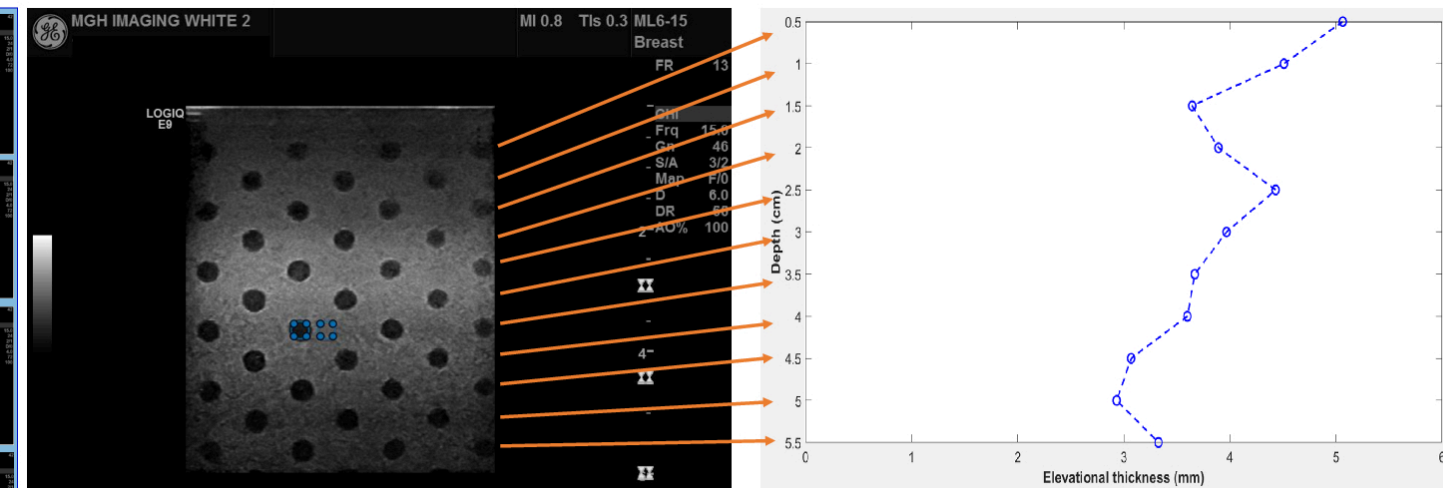


Figure 4. Image obtained using a ML6-15-D on a GE Logiq E9, three transmit focal zones (Left: Sono408 phantom; Right: Estimated elevational beam thickness for various depths calculated based on the B-mode image of this phantom using ROIs in the lesion and in the background area.)

The left side of figure 4 is a B-mode image of the Sono408 phantom, taken using scan parameters based on a “Breast” protocol for an ML6-15-D transducer connected to a GE Logiq E9 scanner. Three transmit focal zones were utilized, with the deepest one located at 6cm and the shallowest at a little less than 3cm. ROIs of equal size were selected for each depth, one within a spherical lesion at that depth and one within the neighboring background area. The latter is typically to the right of the corresponding lesion, although data has shown that choosing this ROI to the left of the lesion will not change the elevational thickness estimation by more than 6.6% for all depths used here. The right plot of figure 4 shows the estimated elevational beam width (slice thickness) as a function of depth. For the transmit focus conditions, slice thickness is estimated to be 5.1mm at the shallow depth (0.5cm); it gradually decreases with depth until the depth is 1.5cm; it then increases with depth until the depth reaches 2.5cm. Beyond 2.5cm the estimated slice thickness decreases, reducing to 2.9mm at a depth of 5cm. It then starts to increase again. Such a change of slice thickness with depth likely indicates that a narrow row configuration (in the elevational direction) of the matrix array is used in near field (≤ 2.5 cm), and a broad row configuration is used in the far field (≥ 2.5 cm).

The calculation of elevational thickness using the prototype, random void phantom is a little more difficult, but can still be done by scanning the probe across its surface to acquire a cine loop, then figuring out which frame captures the main part of the lesion that will be used to calculate the elevational thickness for the corresponding depth.

CONCLUSIONS

The prototype phantom with randomly distributed anechoic spheres showed similar patterns of lesion detectability as the Sono408 phantom when scanned with 1.25D probes. These phantoms could be very useful for evaluating lesion detectability of transducers, establishing presets on scanners, and transducer and system comparisons.

ACKNOWLEDGEMENTS

We sincerely thank Melanie Orlowski from Massachusetts General Hospital for providing the Ultrasound scanners used for this project.

CONTACT INFORMATION

Zhimin.li@nm.org

REFERENCES

1. Jian-Feng Chen, James Zagzebski, Cristel X Baiu, Zhimin Li. Estimating elevational beam widths by modeling contrast-to-background echo signal intensity on images of anechoic spherical targets in an echogenic background. (in preparation.)